INTERNATIONAL JOURNAL OF BIOASSAYS
ISSN: 2278-778X
CODEN: IJBNHY
ORIGINAL RESEARCH ARTICLE
OPEN ACCESS

KINETIC STUDY, CHARACTERIZATION AND THEORETICAL STUDIES OF OXIDATIVE CHEMICAL POLYMERIZATION OF PARA-AMINOPHENOL IN ACID MEDIUM USING $K_2CR_2O_7$ AS OXIDIZING AGENT

Sayyah SM[1*], Moustafa H[2], El-Ghandour AH[1], Aboud AA[3] and Ali MY[1]
[1]Chemistry Department, Faculty of Science, BeniSuef University-62514 Beni-Suef, Egypt.
[2]Chemistry Department, Faculty of Science, Cairo University, Egypt.
[3]Physics Department, Faculty of Science, Beni Suef University-62514, Beni-Suef, Egypt.

Received for publication: March 18, 2015; **Accepted:** April 13, 2015

Abstract: The synthesis of poly-p-aminophenol (PPAP) by oxidative chemical polymerization using potassium dichromate as oxidizing agent was carried out. The optimum conditions for the polymerization reaction were investigated. The order of reactions and thermodynamic activation parameters were calculated. A molecular mechanism for the oxidation of p-aminophenol using potassium dichromate is proposed. This mechanism explains the specific features of p-aminophenol oligomerization and polymerization reactions. Spectroscopic studies using IR, UV–vis and elemental analysis have evidenced the structure of polymeric chain. The surface morphology of the obtained polymer was characterized by X-ray diffraction and transmission electron microscopy (TEM). The thermo gravimetric analysis (TGA) was used to confirm the proposed structure and number of water molecules in each polymeric chain unit. Moreover, determinations of dielectric properties of the prepared polymer at the investigated optimum condition were carried out. The a.c conductivity (σ_{ac}) of (PPAP) was investigated as a function of frequency and temperature. The microscopic conduction mechanism of charge carries over the potential barrier in polymer backbone was found to be classical hopping model. The equilibrium ground state geometric parametric of p-aminophenol (PAP) neutral monomer and radical cation are investigated theoretically using DFT – B3LYP/ 6-311G** level of calculation. The initiation and propagation steps of oxidative chemical polymerization are theoretically investigated.

Key words: oxidative chemical polymerization, p-aminophenol characterization, DFT calculations, electrical conductivity.

INTRODUCTION

Conducting polymers have some similarities to conventional polymers, but the extensive main-chain π-conjugation, which radical increases the chain stiffness, strongly determines its physical properties [1]. The first basic group consists of linear unsubstituted conducting polymers with a stiff (rigid-rod) chains like poly (acetylene) or poly (thiophene) or semi flexible (rods) chains like polyaniline [2]. 4-Aminophenol has highly toxic and mutagenic effects and induces DNA cleavage in mouse and human lymphoma cells [3,4]. Aminophenols are interesting electrochemical materials since, unlike aniline [5] and other substituted anilines [6], they have two groups (–NH_2 and OH), which could be oxidized. Therefore, they could show electrochemical behavior resembling anilines [7] and/or phenols [8,9]. So aminophenols use in many applications as the sensor were prepared by electrochemical polymerization of p-aminophenol in the presence of glucose oxidase on Pt substrates in a KCl solution at a potential of 0.6 V (vs. Ag/AgCl) [10].

Various chemical oxidizing agents, such as potassium dichromate, potassium iodate, ammonium persulphate, hydrogen peroxide, ceric nitrate, ceric sulphate, and ferric chloride have been used for the chemical oxidative polymerization of aniline [11,12].

The aniline derivatives which prepared chemically are almost all donating substitution on benzene ring as (alkyloxy, hydroxy, chloroaniline, etc.,) and also at the nitrogen atom was reported by S.M. Sayyah *et al.,* [13,14,15,16] to improve the solubility of polyaniline. The kinetics of chemical polymerization of 3-methylaniline, 3-chloroaniline, 3-hydroxyaniline , 3-methoxyaniline and N-methyl aniline in hydrochloric acid solution using potassium dichromate as oxidant and characterization of the polymer obtained by IR, UV-visible and elemental analysis, X-ray diffraction, scanning electron microscopy, TGA-DTA analysis and a.c conductivity have been reported by S.M.Sayyah *et al.,* [17,18,19].

The present works contains theoretical and kinetic studies of the oxidative chemical polymerization using potassium dichromate as oxidant for p-aminophenol monomer in aqueous HCl medium. The obtained polymer is characterized by IR, UV-visible, TGA, elemental analysis, X-ray, transmission electron microscopy (TEM) and a.c conductivity measurements.

MATERIALS AND METHODS

P-aminophenol provided by Honeywell Chemical Co., (Germany). Concentrated hydrochloric acid, pure grade product, provided by El-Nasr pharmaceutical chemical Co., Egypt. Potassium dichromate provided by Sigma-Aldrich chemical Co., (Germany). Doubly distilled water was used to prepare all the solutions needed in the kinetic studies.

***Corresponding Author:**
S. M. Sayyah,
Chemistry Department,
Faculty of Science,
BeniSuef University-62514,
Beni-Suef, Egypt.

Oxidative Aqueous Polymerization of p-Aminophenol Monomer

The polymerization reaction was carried out in a well-stoppered conical flask of 100 ml capacity; addition of p-Aminophenol monomer (PAP) amount in 15 ml HCl of known molarity followed by addition of the required amount of potassium dichromate as oxidant in water (10 ml) to the reaction mixture. The orders of addition of substances were kept constant in all the performed experiments. The stoppered conical flasks were then placed in an automatically controlled thermostat at the required temperature. The flasks were shaken (15 shakings/ 10s /30 min) by using an automatic shaker. The flasks were filtrated using a Buchner funnel, and then the obtained polymer was washed with distilled water, and finally dried till constant weight in vacuum oven at 60°C.

Calculations

Determination of Conversion Yield: The conversion yield of the monomer to the polymer was determined by the weighing of the dry obtained polymer (P) divided by the weight of the monomer (w) and was calculated in the following way:

$$\text{Conversion yield \%} = \frac{Polymer\ Yield\,(P)}{Weight\ of\ Momoner\ (w)} \times 100 \quad (1)$$

Determination of the Polymerization Rate: The rate of polymerization was determined by the following equation:

$$\text{Rate}\,(R_i) = \frac{P}{\text{V x M. wt xt}}\ (\text{gm ol / L. sec}) \quad (2)$$

Where (P) is the weight of polymer formed at time (t) in seconds, (V) is the volume of the reaction solution in liters and (M.wt) is the molecular weight of the monomer [20].

Calculation of the Apparent Activation Energy: The apparent activation energy (E_a) of the aqueous polymerization reaction was calculated using the following Arrhenius equation:

$$\text{Log(K)} = \frac{-Ea}{2.303RT} + C \quad (3)$$

where (K) is the rate, (R) is the universal gas constant, T is the reaction temperature and (C) is constant [21].

Determination of Enthalpy (Δ H*) and Entropy (ΔS*): Enthalpy of activation (ΔH^*) and entropy (ΔS^*) were calculated using transition state theory equations (Eyring equation):

$$K = \frac{KT}{Nh} e^{\Delta S^*/R} . e^{-\Delta H^*/RT} \quad (4)$$

where (K) is the rate constant, (N) is the Avogadro's number, (R) is the universal gas constant and h is planks constant.

By dividing the above equation by (T) and taking its natural logarithm, the following equation obtained:

$$\text{Ln}\left(\frac{K}{T}\right) = Ln\frac{R}{Nh} + \frac{(\Delta S^*)}{R} + \frac{(-\Delta H^*)}{RT} \quad (5)$$

A plot of Ln (k/T) against (1/T) is linear, with a slope equals to ($-\Delta H^*/R$) and intercept equals to (Ln. k/h + $\Delta S^*/R$). Therefore (ΔH^*) and (ΔS^*) can be calculated from the slope and intercept, respectively [20,21].

Elemental Analysis, Infrared and Ultraviolet Spectroscopy:

The carbon, hydrogen and nitrogen contents of the prepared polymer was carried out in the micro analytical laboratory at Cairo University by using oxygen flask combustion and a dosimat E415 titirator (Switzerland).

The infrared spectroscopic analysis of the prepared polymer at the investigated optimum condition was carried out in the micro analytical laboratory at Cairo University by using a Shimadzu FTIR-430 Jasco spectrophotometer using KBr disc technique.

The ultraviolet-visible absorption spectra of the monomer and the polymer sample prepared at the optimum conditions were measured using Shimadzu UV spectrophotometer (M 160 PC) at room temperature in the range 200-400 nm using dimethyl formamide as a solvent and reference.

Thermal Gravimetric Analysis (TGA), Transmission Electron Microscopy (TEM) and X-Ray Analysis:

Thermal gravimetric analysis (TGA) of the polymer sample was performed using a SHIMADZU DT-30 thermal analyzer. The weight loss was measured from ambient temperature up to 600 °C at rate of 20 °C/ min to determine the rate of polymer degradation.
X-Ray diffractometer (philip1976.model1390) was used to investigate the phase structure of the polymer powder under the following condition which kept constant during the analysis processes:

X-ray tube: Cu: scan speed =8/min: current=30mA: voltage =40kv: and preset time=10s.

The inner cavity and wall thickness of the prepared polymer was investigated using transmission electron microscopy (TEM) JEOL JEM-1200 EX Π (Japan).

Dielectric properties and a.c conductivity Measurements:

The dielectric constant (έ), the dielectric loss (ε'') and a.c conductivity (σ_{ac}) were measured using Philips RCL bridge (digital and computerized) at a

frequency range 12 - 10^5 Hz and over temperature range 30 – 60°C.

The values of the dielectric constant were determined using standard geometric technique in which the capacitance (C) was assumed to be given by the usual expression for a parallel plate capacitor. Using the following equation:

$$\acute{\varepsilon} = \frac{Cd}{\varepsilon_0 A} \quad (6)$$

where (έ) is the dielectric constant, (ε_0) is the permittivity of vacuum, A is the area of the sample and d is the sample thickness.

The dielectric loss (ε'') was calculated from the measurements of the loss factor (D) and (έ) using the following relation:

$$\varepsilon'' = D\,\acute{\varepsilon} \quad (7)$$

The ac conductivity was measured using Philips RCL Bridge (digital and computerized) at a frequency range 0.1 – 100 k Hz and at temperature range 30 – 80 °C. The temperature was controlled by the use of a double wound electric oven.

The a.c conductivity (σ_{ac}) value was calculated using the following relation:

$$\sigma_{ac} = \varepsilon'' \omega \varepsilon_0 \quad (8)$$

where ω = 2πf and f is the applied frequency.

Method of calculations

In this work DFT (B3LYP) [22,23] method was used. This functional is a combination of the Becke's three parameters non-local exchange potential with the non-local correlation function of Lee *et al.*, Full geometry optimization was performed using 6-311G (d,p) as a basis set to generate the optimized structures and ground state properties of p-aminophenol, radical cation (monomer and dimmer…etc.). All calculations were performed using Gaussian 09 W program [24].

RESULTS AND DISCUSSION

Determination of the Optimum Polymerization Conditions

The polymerization process of p-aminophenol (PAP) occurs by using hydrochloric acid (HCl) as dopant and acid medium in the presence of potassium dichromate as oxidizing agent at 15±0.2 °C for one hour, using constant total volume (25 ml). The obtained yield of the polymer was determined after drying under vacuum at 60°C until constant weight.

Effect of the Monomer Concentration

The effect of monomer concentration on the aqueous oxidative polymerization of p-aminophenol (PAP) was investigated using constant concentration of $K_2Cr_2O_7$ at 0.2M and HCl concentration at 0.3M by using different concentration of p-aminophenol (PAP) at 15 ± 0.2◦C. The yield-time curve was represented in Figure (1), from which it is clear that the obtained yield increases with the increase of p-aminophenol concentrations in the range from 0.1 to 0.4 then decreases gradually up to 0.5M. This behavior may be due to, at higher concentration of HCl, the degradation of the polymer in the early stages of the reaction, which may be due to the hydrolysis of (PPAP) chains [25].

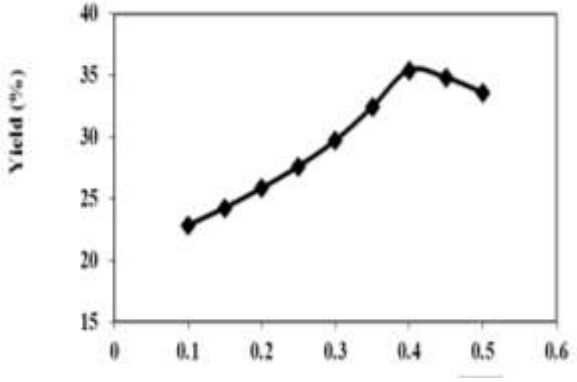

Figure 1: Yield - monomer concentration effect on the aqueous chemical oxidative polymerization of (PPAP).

Effect of HCl Concentration

To study the effect of HCl concentration on the polymerization reaction, both oxidant ($K_2Cr_2O_7$) and monomer concentrations were fixed at 0.2 and 0.4 M respectively while but HCl concentration was varied from 0.1 M to 0.5 M at 15±0.2°C. The relation between (PPAP) yield and different concentrations of HCl is represented in figure (2). From which it is clear that, the polymer yield increase with the increasing of acid concentration in the range from 0.1 to 0.3 then decreases gradually up to 0.5M.

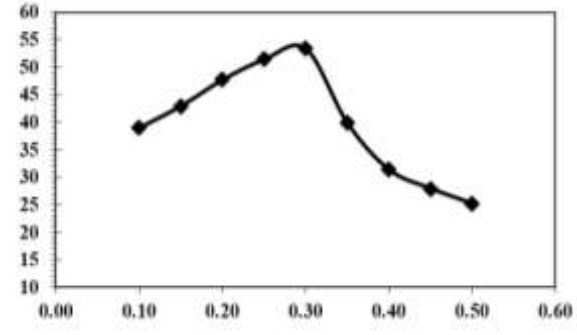

Figure 2: Yield - HCl concentration effect on the chemical polymerization of (PPAP).

Effect of Potassium Dichromate Concentration

Both of the monomer and HCl concentrations are kept constant at 0.4 and 0.3 M respectively while the oxidant concentrations were varied from 0.1 to 0.5M at 15±0.2°C to investigate the optimum polymerization condition of oxidant. Figure (3) shows the plot of polymer yield of (PPAP) against different concentrations of the oxidant. The obtained yield increases with the increase of $K_2Cr_2O_7$ concentration reaching maximum value at 0.3M then decreases from 0.3M to 0.5M. In the first part of the curve the produced initiator ion radical moieties activate the backbone and consequently produce the p-aminophenol (PAP) ion radical, which takes place immediately and therefore, the yield increases with the increase of potassium dichromate concentration up to 0.3M. But in the range from 0.3M to 0.5M the polymer yield decrease, may be due to at a high concentration of oxidant, it promotes the formation of low molecular weight oxidation product and also may be degrade the produced polymer which is easily soluble in acid medium [21,25].

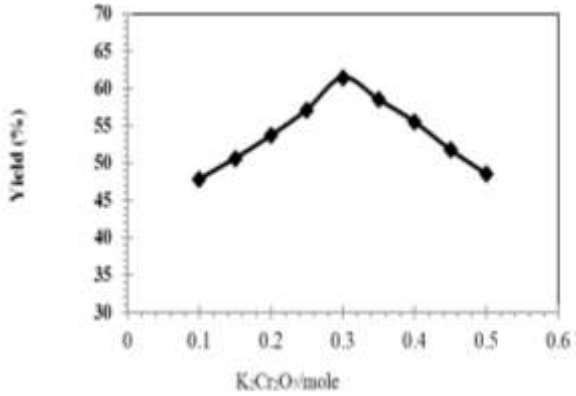

Figure 3: *Yield - $K_2Cr_2O_7$ concentration* effect on the aqueous chemical oxidative polymerization of (PPAP).

The kinetic Studies of the Polymerization Reaction

Effect of Monomer (PAP) Concentration: The effect of monomer concentration on the aqueous oxidative polymerization of PAP is investigated by using different concentrations of monomer (0.05-0.4 mol/L) at constant volume 25 ml. The HCl solution and potassium dichromate concentrations were fixed at 0.3 M and 0.3 M respectively at 15 ±0.2 °C for different time intervals. The yield-time curve is plotted for each monomer concentration and the data are graphically represented in figure (4-a). The monomer exponent was determined from the slope of the straight line represented in figure (4-b) for the relation between log R_i and logarithm of the monomer concentration. The slope of this linear relationship is found to be 0.98 which means that the polymerization reaction with respect to the monomer concentration is a first order reaction.

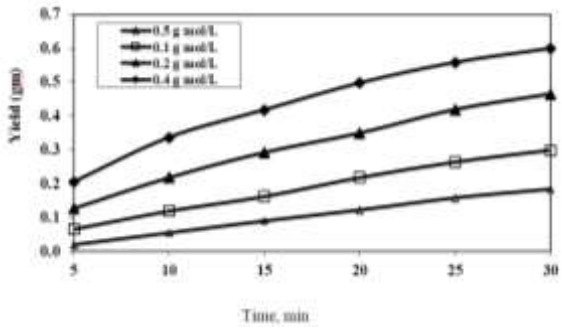

Figure 4a: Conversion -monomer/mol concentration effect on the aqueous oxidative polymerization of (PAP) at different time intervals.

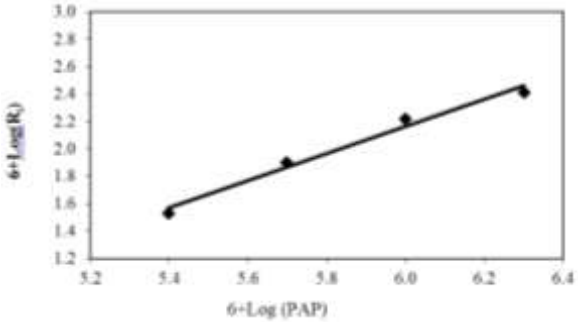

Figure 4b: Double logarithmic plot of the initial rate and monomer concentration of (PAP).

Effect of hydrochloric Acid Concentration: The kinetic study of the aqueous oxidative chemical polymerization for (PAP) was carried out using constant monomer concentration at (0.4 M) and $K_2Cr_2O_7$ as oxidant at (0.3 M) using different molarities from HCl (0.05 - 0.3 mol/L) and constant total volume (25 ml) at 15 ±0.2°C for different time intervals. The yield-time curves were plotted for each acid concentration used as shown in figure (5-a). From which it is clear that, both the initial and overall reaction rates of the polymerization reaction increase with the increasing of HCl concentrations in the range between 0.05-0.3 mol/L. The HCl exponent was determined from the relation between logarithm of the initial rate of polymerization (log (R_i)) against logarithm of the HCl concentration as represented in figure (5-b). A straight line is obtained with a slope equal to 1.024, which means that the polymerization reaction is a first order reaction with respect to HCl concentration.

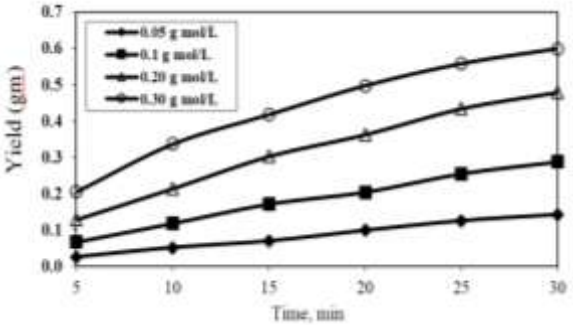

Figure 5a: Yield -time curve for the effect of HCl concentration on the Polymerization of p-aminophenol (PAP) at different time intervals.

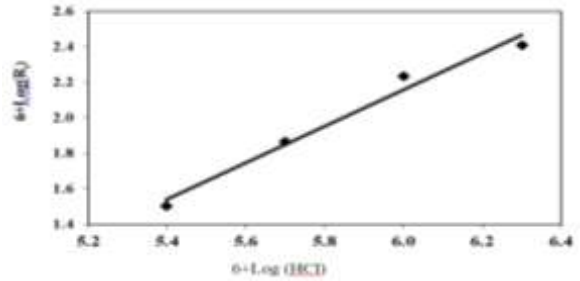

Figure 5-b: Double logarithmic plot of the initial rate and HCl concentration for the chemical oxidative polymerization of (PAP).

Effect of Potassium Dichromate Concentration: The effect of $K_2Cr_2O_7$ on the aqueous chemical oxidative polymerization of (PAP) was carried out at fixed concentrations of monomer at 0.4 M and HCl at 0.3 M. The oxidant concentration was investigated in the range between 0.05-0.3 mol/L using constant total volume (25 ml) at 15 ±0.2°C for different time intervals. The yield-time curves were plotted for different oxidant concentrations and the data are graphically represented in figure (6-a). The initial and overall reaction rates were determined using equation (2). Figure (6-a) shows that, the initial and overall reaction rate of the polymerization reaction increases with the increase of oxidant concentration in the range between 0.05 - 0.3 mol/l. The oxidant exponent was determined from the relation between logarithm of the initial rate of polymerization (log (R_i)) against logarithm of the oxidant concentration. A straight line was obtained with a slope of 1.12 as represented in figure (6-b). This means that the polymerization reaction of (PAP) is a first order reaction with respect to the oxidant.

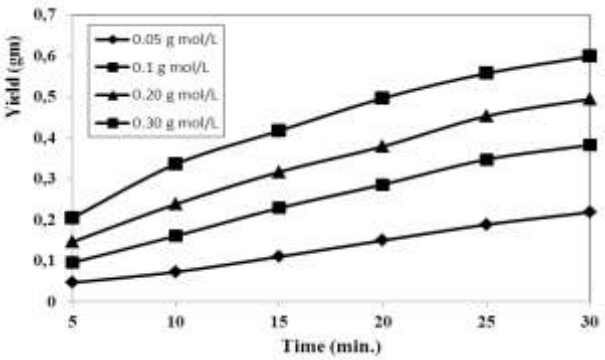

Figure 6a: Yield-time curve for the effect of potassium dichromate concentration on the polymerization of (PAP) at different time intervals.

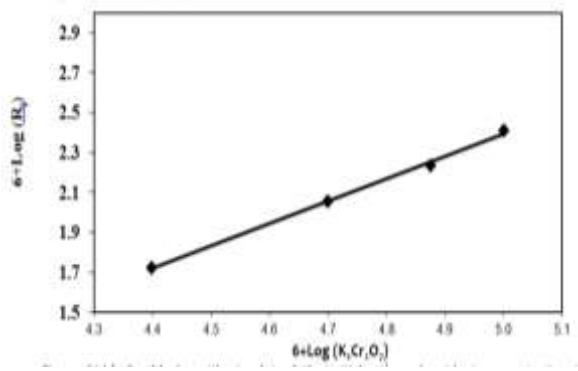

Figure 6b: Double logarithmic plot of the initial rate and oxidant concentration in case of polymerization of (PAP).

Calculation of the Thermodynamic Activation Parameters

The aqueous oxidative polymerization of 0.40 mol/L (PAP), 0.3 mol/L HCl and 0.3 mol/L potassium dichromate as oxidant was carried out at 5, 10 and 15 °C for different time intervals. The yield- time curves were plotted in figure (7), from which it is clear that both of the initial and overall reaction rates increase with raising the reaction temperature. The apparent activation energy (E_a) of the aqueous polymerization reaction was calculated using equation (6). The apparent activation energy for this system was found to be 89.24 kJ/mol. The enthalpy and entropy of activation for the polymerization reaction can be calculated by the calculation of K_2 from the following equation:

$$\text{Reaction Rate} = K_2\,[\text{oxidant}]^{1.121}\,[\text{HCl}]^{1.024}\,[\text{monomer}]^{0.984} \quad (9)$$

The values of K_2 at 5, 10 and 15 °C were 2.07 x 10^{-6}, 4.32 x 10^{-6} and 7.89 x10^{-6} respectively. The enthalpy (ΔH^*) and entropy (ΔS^*) of activation associated with K_2, were calculated using Eyring equation (4).

Where K_2 is the rate constant, N is the Avogadro's number, R is the universal gas constant and h is planks constant.

Figure 9 shows the relation between K_2/T vs 1/T, which gives a linear relationship with slope equal to ($-\Delta H^*$)/R and intercept equal to (log R/Nh +ΔS^*/R). From the slope and intercept, the values of ΔH^* and ΔS^* are calculated and found to be equal to 86.88 kJmol^{-1}, and -127.93 Jmol^{-1}K^{-1} respectively.

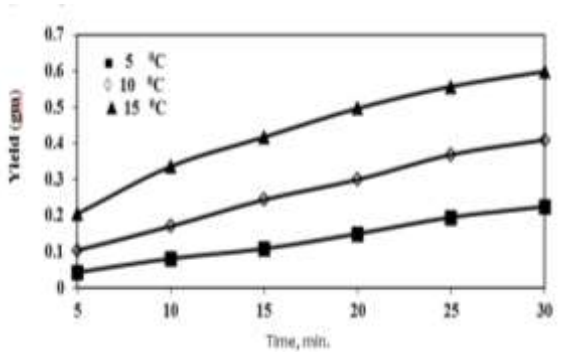

Figure 7: Yield -time curve for the effect of temperature on the aqueous oxidative polymerization of (PAP).

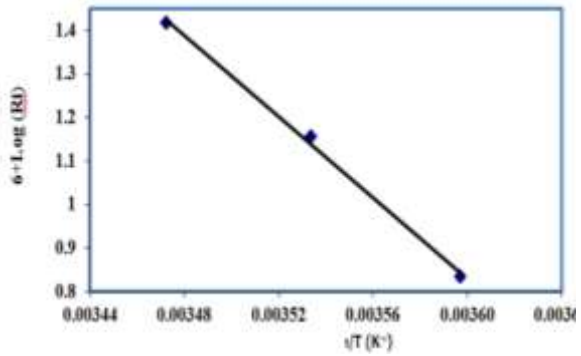

Figure 8: The relation between the logarithm of initial rate and (1/T) for aqueous chemical oxidative polymerization of (PAP).

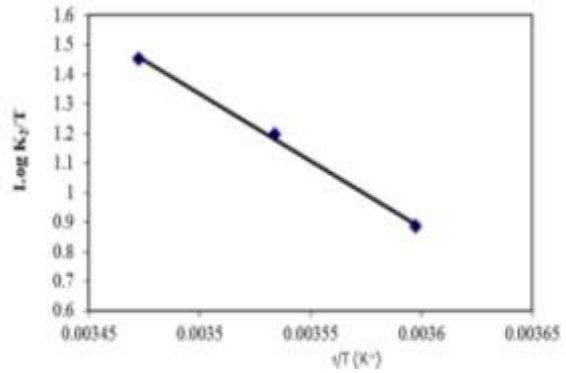

Figure 9: The relation between log K_2/T and 1/T for the polymerization reaction of (PAP).

Polymerization Mechanism

The aqueous chemical oxidative polymerization of (PAP) is described in the Experimental section and follows three steps [21, 25]:

The Initial Step

Potassium dichromate in acidified aqueous solution produces chromic acid as shown in equation (10):

$$K_2Cr_2O_7 + H_2O + 2H^+ = 2K^+ + 2H_2CO_4 \quad (10)$$

This reaction is controlled by the change in pH, the orange red dichromate ions $(Cr_2O_7)^{2-}$ are in equilibrium with the $(HCrO_4)^-$ in the range of pH-values between 2 and 6, but at pH below 1 the main species is (H_2CrO_4) and the equilibrium can occur as follows:

$$(HCrO_4)^- \rightleftharpoons (CrO_4)^{2-} + H^+ \quad K= 10^{-5.9} \quad (11)$$

$$(H_2CrO_4) \rightleftharpoons (HCrO_4)^- + H^+ \quad K= 4.1 \quad (12)$$

$$2(HCrO_4)^- \rightleftharpoons (Cr_2O_7)^{2-} + H_2O \quad K= 10^{-2.2} \quad (13)$$

The chromic acid withdraws one electron from each protonated PAP and probably forms a metastable complex as shown in equation (14):

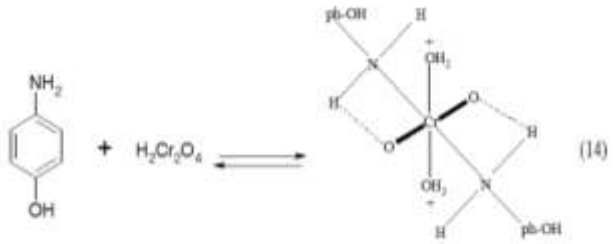

(14)

The complex undergoes dissociation to form monomer radical cation. Part from radical cation form the dimmer then trimmer and etc., and another part go to in another pathway where it form 1,4 benzoquinone which is soluble in the medium of the reaction [26] as shown in equation (15):

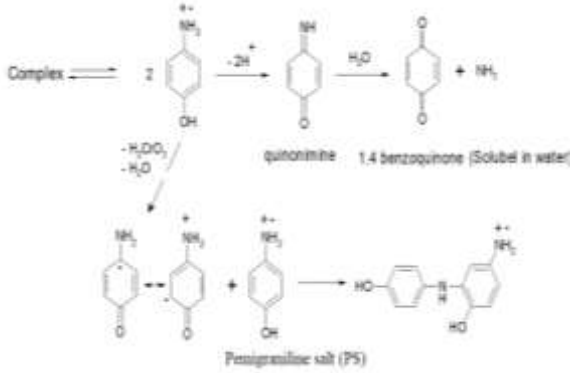

Scheme 1: Proposed mechanism of aqueous chemical oxidative polymerization of p-aminophenol.

Generally, the initial step is rapid and may occur in short time, 0–5 min (autocatalytic reaction).

Propagation Step:

This step involves the interaction between the formed radical cation and the monomer to form a dimer radical cation. In the case of Cr (VI) oxidation of the organic compounds, Cr (VI) is reduced to Cr (IV) first and then to Cr (III) [20,22]. Transfer of two electrons from two monomer ion radical by H_2CrO_4 produces parasemidine salt along with chromous acid $H_2Cr_2O_3$ (Cr (IV)). The intermediately produced Cr (IV) oxidizes parasemidine to pemigraniline salt (PS) at suitable low pH and the PS acts as a catalyst for conversion of p-aminophenol to poly-p-aminophenol.

In case of PPAP the para position is busy so, the polymerization occurs in the meta position.

This reaction is followed by further reaction of the formed dimmer radical cations with other monomer molecules to form trimer radical cations and so on. The degree of polymerization depends on different factors such as oxidant concentration, HCl concentration, monomer concentration, and temperature. By adding equations 9, 13, 14 and 15:

$$2(NH3)\text{-}ph\text{-}OH + K_2Cr_2O_7 + 8\ H^+ = PS + 2K^+ + 2Cr^{3+} + 7H_2O \quad (16)$$

$$12\ PPAP + 5\ K_2Cr_2O_7 + 34\ H^+ = 6\ PS + 10\ Cr^{3+} + 10\ K^+ + 35\ H_2O \quad (17)$$

Termination Step

Termination of the reaction occurs by the addition of ammonium hydroxide solution in an equimolar amount to HCl present in the reaction medium (till pH = 7), which leads to the stopping of the redox reaction. The reaction could occur as follows:

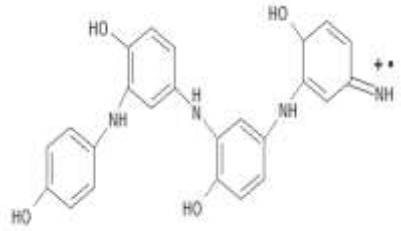

DFT Calculations

From the polymerization mechanism see (Section 3.4), the radical cation formed in the initial step (0-5 min) followed by the propagation step involves the interaction between the formed radical cation and the monomer to form a dimmer radical cation. This reaction is followed by further reaction to form the polymer chain. In this section, by the theoretical calculation we can explain why radical cation start the polymerization and not the neutral monomer of p-aminophenol and at the same time explore the stability of the dimmer radical cation if it is (ortho or meta) – position in the propagation steps.

Monomer and radical cation (initiation)

The final optimized geometry, numbering system, the vector of the dipole moment, the equilibrium bond length and net charge on active center of neutral monomer and radical cation of p-aminophenol using DFT – B3LYP/ 6-311G** are present in figure (10 and 11). Table (1) present the total energy (E_T), E_{HOMO}, E_{LUMO}, energy gap (E_g) and dipole moment of neutral and radical cation of p-aminophenol.

Table 1: The total energy (E_T), energy of HOMO, LUMO, energy gap (E_g) and vector of the dipole moment (μ) of the monomer and the radical cation of (PAP).

Parameter	Monomer	Radical cation
E_T (a.u)	-362.9317	-362.6729
E_{HOMO} (a.u)	-0.19912	-0.39882
E_{LUMO} (a.u)	-0.01874	-0.32357
E_g (eV)	4.9084	2.0476
Total μ (D)	2.1247	3.4296

Some general remarks can be considered:

1. The computed total energy of radical cation is less stable then neutral monomer by 7.04 eV (162.40 kcal), indicating that the radical cation is more reactive than neutral monomer.
2. The computed energy gap (E_g), which measure the reactivity, as the energy gap decrease the reactivity increase. In our case the E_g of radical cation is less than the neutral monomer by 2.86 eV (65.97 kcal), the second reason why radical cation is more reactive and starting the process of polymerization.
3. From the computed dipole moment, it is found that the dipole moment of radical cation is greater than the neutral monomer by 1.31D.
4. The net charge on N-atom of amino group in neutral monomer is -0.318 e whereas, in radical cation is -0.218 e. The decrease in negativity of N-atom of amino group is another reason for this center to attack the ortho- or meta–position of the neutral monomer to start polymerization as indicated in HOMO charge density map (Fig. 10, 11).

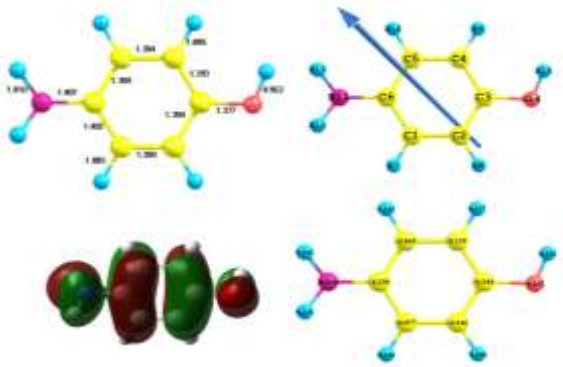

Figure 10: Optimized structure, numbering system, vector dipole moment, bond length, net charge and HOMO charge density of the monomer (PAP).

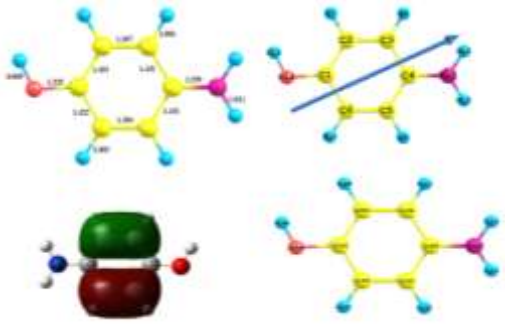

Figure 11: Optimized structure, numbering system, vector dipole moment, bond length, net charge and HOMO charge density of (PAP) radical cation.

Propagation step

The next step of the polymerization is the propagation step at which the radical cation attacks another monomer to form the dimmer radical cation.

To prove which position in the monomer attack by the radical cation to form the dimmer radical cation is to calculate the total energy of the dimmer radical cation at B3LYP/ 6-311G** method. Figure 12 Presents the final geometry, the vector of the dipole moment, total energy and energy gap and HOMO charge density maps. Two possible structures may be consider, dimmer radical cation (ortho- attack) and dimmer radical cation (meta-attack). From figure 12 and table 2 one can reveal the following:

1. The computed total energy (E_T) (which measure the stability of any compound) of dimmer radical cation (meta-attack) and dimer radical cation (ortho-attack) are of the same order ≈ 1 kcal /mole so, both species exists in the reaction medium.
2. But on other hand the computed energy gap (E_g) of dimmer radical cation (meta- attack) is less (more reactive) than (ortho- attack) by 25 kcal, as the energy gap decrease, the reactivity increase. Therefore, the dimmer radical cation (meta-attack) is more reactive and more favorable than dimer radical cation (ortho-attack) in the propagation process.

Dimmer radical cation (meta-attack) interacts with another monomer to form trimmer and so on to form polymer chain scheme (2).

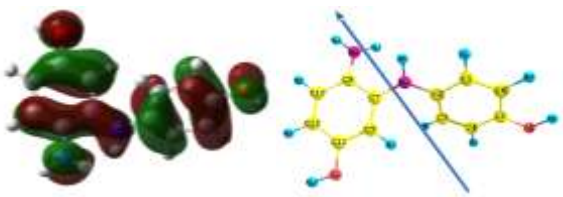

The ortho-position: ***Dimmer***

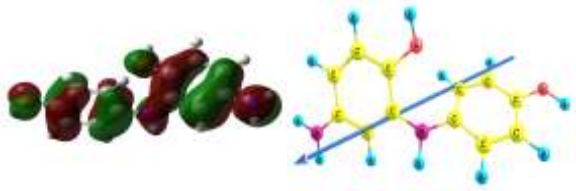

The meta-position

Figure 12: Geometry optimization, vector dipole moment and HOMO charge density of ortho- and meta-position of the dimmer.

Table 2: The total energy (E_T), energy of HOMO, LUMO, energy gap (E_g) and vector of the dipole moment (μ) of (ortho and meta) – position of the dimmer.

Parameter	ortho-position	meta-position
E_T (a.u)	-720.3064	-720.3048
E_{HOMO} (a.u)	-0.3289	-0.3195
E_{LUMO} (a.u)	-0.2743	-0.2707
Eg (e.v)	1.4863	1.2274
Total μ (D)	5.2486	4.1100

Characterization of the Obtained Polymer

The Elemental Analysis: The data obtained from elemental analysis using oxygen flask combustion and a dosimat E415 titirator which are given in table (2) shows that, the found carbon content of (PPAP) is lower than the calculated value. This is due to the formation of chromium carbide during step of heating and measuring process while the found value of nitrogen and hydrogen are 8.62 and 4.26 respectively which are in good agreement with the calculated one for the suggested structure present in scheme (2). By measuring another sample of the (PPAP) which was prepared by using ammonium persulfate as oxidant the found value of carbon, is higher than sample which, is prepared by using potassium dichromate as oxidant [21,27].

Table 3: The elemental analysis of poly-P-aminophenol (PPAP).

C %		N %		H %	
Calc.	Found	Calc.	Found	Calc.	Found
51.16	35.89	9.55	8.62	4.64	4.26

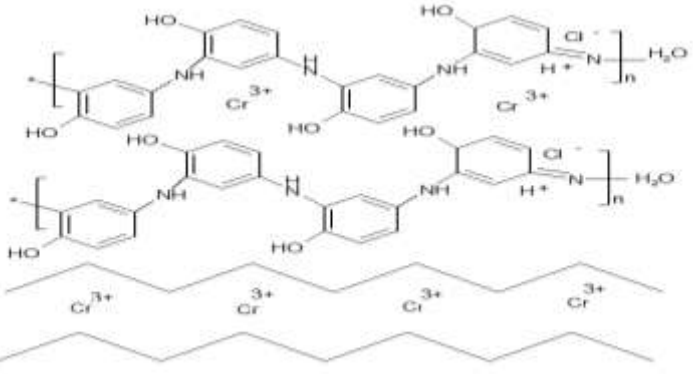

Scheme 2: Structure of the prepared poly p-aminophenol (PPAP)

The infrared spectroscopic analysis of (PPAP) monomer and its analogs polymer

The IR spectra of the p-aminophenol (PAP) and its polymer (PPAP) are represented in Figure (13), while the absorption band values and their assignments are summarized in Table (4). The medium absorption band appearing at 491 cm^{-1} for monomer and the medium absorption band appearing at 525 cm^{-1} in case of polymer may be attributed to the torsional oscillation of NH^{3+} group. The strong absorption band appearing at 740 cm^{-1} may be due to the out of plane CH deformation of 1,4-disubstitiation in benzene ring in case of monomer, appears at 750 cm^{-1} with slightly shift in case of polymer. A series of absorption bands appearing in the region from 800 …. 1132 cm^{-1} which could be attributed to out-of-plane bending of C-H bonds of aromatic ring in both cases (monomer and polymer). The medium absorption band appearing at 1220 cm^{-1} which could be attributed to bonding vibration C-O-H in case of monomer, appears at 1275 cm^{-1} with slightly shift in case of polymer. The medium absorption band appearing at 1403 cm^{-1} which may be attributed to bending deformation of C-H group attached to benzene ring in case of monomer, appears at 1420 cm^{-1} with slightly shift in case of polymer. The sharp absorption band appearing at 1509 cm^{-1} which could be attributed to N-H bending deformation in case of monomer, appears at 1556 cm^{-1} with slightly shift in case of polymer.

The sharp absorption band appearing at 1600 cm^{-1} in case of monomer and the shoulder band appearing at 1639cm^{-1} in case of polymer could be attributed to symmetric stretching vibration of C=C in aromatic system or C=N in quinoid structure. The shoulder band appearing at 3015 cm^{-1} which may be due to an overtone of the N–H bending vibration in case of monomer, disappear in case of polymer. The sharp absorption bands appears at 3202 and 3373 cm^{-1} which could be attributed to symmetric stretching vibration for –OH and -NH groups in case of monomer, while appearing as a broad band at 3481 cm^{-1} due to the merging of two individual absorption peaks from the stretching vibrations of –OH group and $–NH_2$ group in case of polymer.

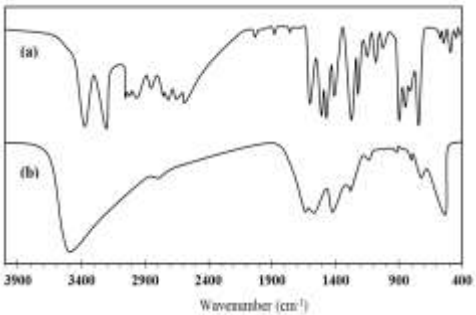

Figure 13: The infrared spectrum of PAP (a) and its polymer (b).

The UV-visible Spectroscopic Study of p- aminophenol monomer and its analogs polymer

The UV-visible spectra of P-aminophenol (PAP) and its polymer (PPAP) are represented in Figure (14); the spectra show the following absorption bands:

(1) In case of monomer, two absorption bands appear at λ_{max} = 215 and 244 nm which may be attributed to π-π^* transition (E_2-band) of the benzene ring and the β-band ($A_{1g} – B_{2u}$).

(2) In case of polymer, the absorption band appear at λ_{max} = 224 and 258 nm which may be attributed to π-π^* transition showing a bathochromic shift. Beside these two bands, broad absorption band appears in the visible region at λ_{max} = 448 nm which may be due to the high conjugation of the aromatic polymeric chains.

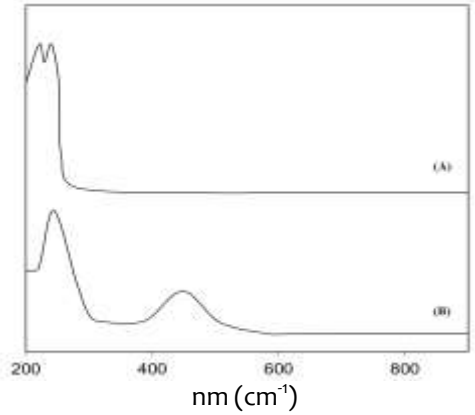

Figure 14: UV-visible spectra of p- tolidine (PAP) (A) and it analogous polymer (PPAP) (B).

Thermal Gravimetric analysis (TGA) of poly p-aminophenol

Thermogravimetric analysis (TGA) for the prepared polymer has been investigated and the TGA-curve is represented in Figure (15). The calculated and found data for the prepared polymers are summarized in table (5). The thermal degradation steps are summarized as follows:

(1) The first stage includes the loss of one water molecule in the temperature range between 36.77-106.91°C the weight of loss of this step was found to be 3.47 % which is in a good agreement with the calculated one 3.41%.

(2) The second stage, in the temperature range between 106.91-186.36°C the weight loss was found to be 6.98 %, which could be attributed to the loss of HCl molecule. The found weight loss is in good agreement with the calculated one (6.89 %).

(3) The third stage, in the temperature range between 186.36-363.46°C, the weight loss was found to be 12.88 %, which is attributed to the loss of four molecules of OH. The calculated weight loss of this stage is equal to 12.79 %.

(4) The fourth stage, in the temperature range between 363.46-522.14°C, the weight loss was found to be 33.83 %, which is attributed to the loss of two molecules of C_6H_3-NH. The calculated weight loss of this stage is equal to 33.72 %.
(5) The fifth stage, in the temperature range between 522.14-687.72°C, the weight loss was found to be 20.45 %, which is attributed to the loss of one molecule of C_6H_3-2NH. The calculated weight loss of this stage is equal to 33.33 %.
(6) The last stage, above 687.72°C, the remained polymer molecule was found to be 22.39 % including the metallic residue but the calculated one was found to be 22.86%.

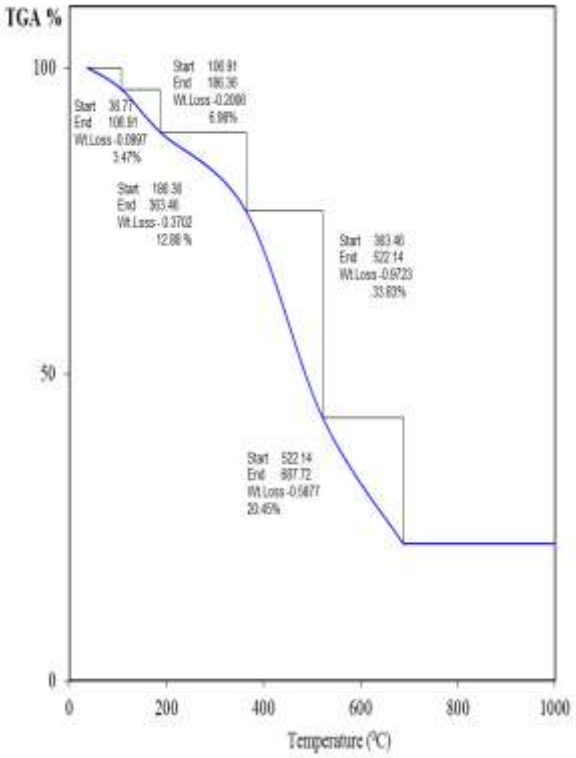

Figure 15: The thermal gravimetric analysis (TGA) for (PPAP).

Table 5: Thermo gravimetric data of PPAP.

Name	Temperature range °C	Weight loss (%)		The removed molecule
		Calc.	Found	
Poly (PAP)	36.77-106.91	3.41	3.47	H_2O
	106.91-186.36	6.89	6.98	HCl
	186.36-363.46	12.79	12.88	4OH
	363.46-522.14	33.72	33.83	$2C_6H_3$+2NH
	522.14-687.72	20.33	20.45	C_6H_3+2NH
	remaining weight(%) above 687.72	22.86	22.39	Remaining weight and metallic residue

The X-Ray diffraction analysis and transimation electron microscope

The X-Ray diffraction Patterns of the prepared polymer is represented in figure (16). The figure shows that, the prepared PPAP is completely amorphous.

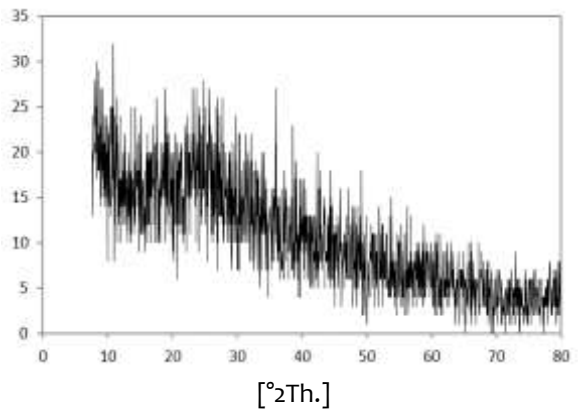

Figure 16: X-ray poly- p- aminophenol (PPAP).

Morphology of PPAP was characterized by transmission electron microscope. Figure (17) shows TEM image of PPAP which shows spherical irregular shape with approximate diameter 93.30-110.20 nm either separated or linked with each other.

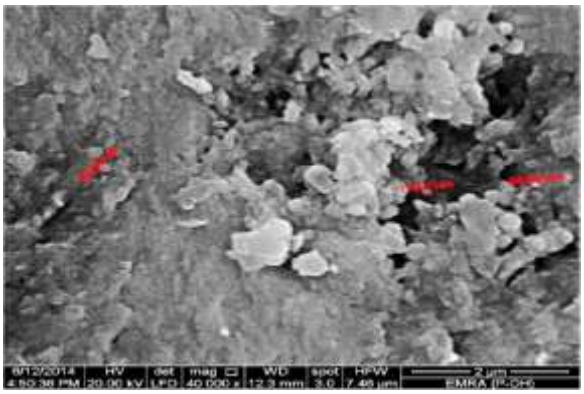

Figure 17: The transimation electron microscope of PPAP

Dielectric properties and a.c conductivity ($\sigma_{a.c}$) measurements

Figure (18) show the variation in dielectric constant (ε) of (PPAP) as a function of frequency. From the figure it is clear that, the dielectric constant decrease sharply up to a certain frequency after which becomes nearly constant. This behavior has also been observed by Rahaman, M, Sohi, N [28,29] and Pant, H.C [30]. This phenomenon could be attributed to relaxation process due to rotational displacement of molecular dipole under the influence of alternating filed which lead to dielectric relaxation. Consequently, decrease in dielectric constant may be due to the contribution of orientation relaxation of dipoles and conduction of charge carriers at higher frequency [31]. This can be explained on the basis of the fact that at close to high frequency, field reversal becomes so fast that dipoles are unable to orient themselves and intrawell hopping probability of charge carriers dominates in rapid field reversal in such a small interval of time [32].

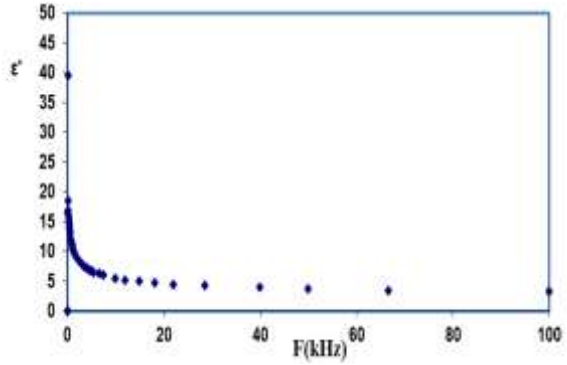

Figure 18: Variation of dielectric constant (έ) of (PPAP) with frequency at room temperature.

Figure (19) reveals that dielectric loss ε″ decrease with the increasing of frequency. A decrease of ε″ orders of magnitude was observed when the frequency was increased from 0.1 kHz to 100 kHz. At low frequency, the high value of dielectric loss ε″ is usually associated with the motion of free charge carriers within the material, dipole polarization or interfacial polarization [32]. At high frequency, periodic field reversal is so fast that there is no excess ion diffusion in the direction of electric field and thus, charge accumulates and polarization decreases due to accumulation of charges leading to the decrease in ε″ [31,33].

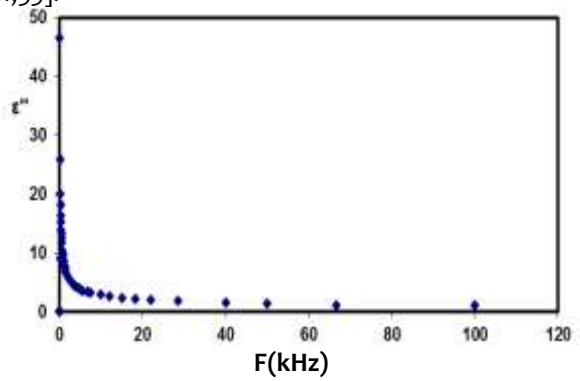

Figure 19: Variation of dielectric loss (ε″) of (PPAP) with frequency at room temperature.

Figure (20) represents the variation in a.c conductivity ($\sigma_{a.c}$) for (PPAP) as a function of frequency and temperature. It is observed that, the value of a.c conductivity increases with the increase of frequency. This behavior is in good agreement with the random free energy model proposed by Dyre, J.C.,[31]. According to this model, conductance increases as a function of frequency in many solids, including polymers, which can be explained on the basis of any hopping model. The rise in conductivity upon increasing the frequency and temperature is common for disordered conducting polymer. As can be seen, each curve displays a conductivity dispersion, which is strongly dependent on frequency and shows weaker temperature dependent.

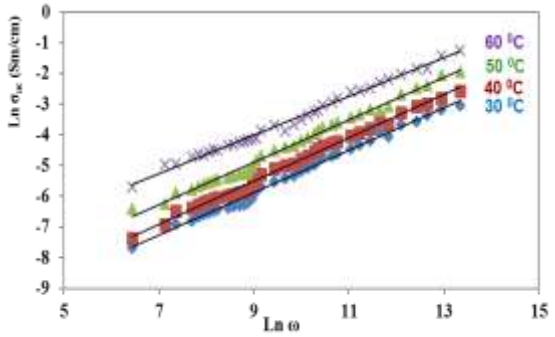

Figure (20): Ac conductivity vs. angular frequency for (PAP) with frequency at different temperatures.

In general, for amorphous conducting material, disordered systems, low mobility polymers and even crystalline materials, the a.c conductivity ($\sigma_{a.c}$) as a function of frequency can be obeys a power law with frequency [34]. The a.c conductivity ($\sigma_{a.c}$) over a wide range of frequencies can be expressed as:

$$\sigma_{a.c}(\omega) = A\omega^{s} \quad (17)$$

Where A is a complex constant and the index (s) is frequency exponent and ω is the angular frequency (ω=2πf).

Figure (21) shows the relation between Ln $\sigma_{a.c}$ and Ln ω at different temperatures. The value of (s) at each temperature has been calculated from the slope of ln σ (ω) versus ln (ω) plot. As shown in figure (21) the calculated value of (s) for (PPAP) sample is less than unity. The microscopic conduction mechanism of disordered systems are governed by two physical processes such as classical hopping or quantum mechanical tunneling of charge carries over the potential barrier separating two energetically favorable centers in a random distribution. The exact nature of charge transport is mainly obtained experimentally from the temperature variation of exponent (s) [35]. The temperature exponent (s) dependences for (PPAP) sample reveals that the frequency exponent (s) decreases with the increase of temperature. This behavior is only observed in the correlated barrier hopping model proposed by Elliott, S. [36].

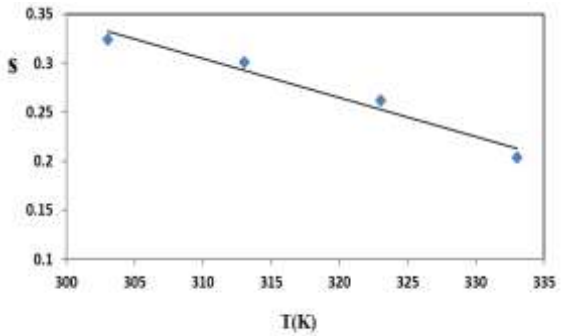

Figure (21):Frequency exponent (s) vs. temperature for poly tolidine.

REFERENCES

1. Skotheim TA, Elsenbaumer RL and Reynolds JR eds. The Handbook of Conducting Polymers, 2nd Ed, (Mercel-Dekker, New York, Basel, Hong Kong, 1997).
2. Genies EM, Boyle A, Lapkowski M, Tsintavis C, Synth. Met. 36(1990)139.
3. Majeska BJ and Holden HE, Environ. Mol. Mutagen. 26 (1995) 163.
4. Yoshida R, Oikawa S, Ogawa Y, Miyakoshi Y, Ooida M, Asanuma K, and Shimizu H, Mutat. Res. 415 (1998) 139.
5. Yang H, Bard AJ, Electroanal J, Chem. 339 (1992) 423.
6. Yamada N, Teshima K, Kobayashi N, Hirohashi R, Electroanal J. Chem. 394 (1995) 71.
7. Chiang J, MacDiarmid A.G, Synth. Met. 13 (1986) 193.
8. Gattrell M, Kirk DW, Electrochem J. Soc. 139 (1992) 2736.
9. Lapuente R, Cases F, Garc_es P, Morall_on E, JL V_azquez JL, Electroanal J. Chem. 451 (1998) 163.
10. Ergun Ekinci, Alev Karagözler A. and Ersin Karagözler A, Electroanalysis Volume 8, Issue 6, pages 571–574, June 1996.
11. Genies, Boyle E, Capkowski A and TsintavisN C, Synth. Met. 36, 139 (1990).
12. Cao Y, Andreatta A, Heeger AJ and Smith P, Polymer 30, 230 (1989).
13. Sayyah SM, Abd El-Salam HM and Azzam EMS, International Journal of Polymeric Materials, vol. 54, no. 6, pp. 541–555, 2005.
14. Sayyah SM, Abd El-Khalek AA, Bahgat AA and Abd El-Salam HA, Polymer International, vol. 50, no. 2, pp. 197–206, 2001.
15. Sayyah SM, Bahgat AA and Abd El-Salam HM, International Journal of Polymeric Materials, vol. 51, no. 3, pp. 291–314, 2002.
16. Sayyah SM and Abd El-Salam HM, International Journal of Polymeric Materials, vol. 52, pp. 1087– 1111, 2003.
17. Sayyah SM, Abd El-Khalek AA, Bahgat AA and Abd El-Salam HM, International Journal of Polymeric Materials, vol. 49, no. 1, pp. 25–49, 2001.
18. Sayyah SM, Abd El-Salam MH and Bahgat AA, International Journal of Polymeric Materials, vol. 51, no. 10, pp. 915–938, 2002.
19. Sayyah SM, Ahmed A Aboud, Amgad B Khaliel and Salama M Mohamed, International Journal of chemistry (2014).
20. Sayyah SM, Aboud AA and Mohamed SM, Hindawi Publishing Corporation International Journal of Polymer Science Volume 2014.
21. Sayyah SM, Ahmed A Aboud, Amgad B Khaliel and Salama M Mohamed, International Journal of Advanced Research volume 2 (2014).
22. Becke D, J. Chem. phys. 98, 1993, 5648-5682.
23. Lee W Yang and Parr RG, Phys. B 37, 1998, 785-789.
24. Gaussian 09, Revision Friseh M.J, Truchs G.W. *et al,*
25. Chowdhury P and Saha B, Indian Journal of Chemical Technology, vol. 12, pp. 671–675, 2005.
26. Horacio J. Salavagione, Joaquin Arias, Pedro Garces *et al,* Journal of Electroanalytical Chemistry (2003).
27. Sayyah SM and Abd El Salam H, International Journal of Polymeric Materials and Polymeric Biomaterials, vol. 55, no. 12, pp. 1075–1093, 2006.
28. Rahaman M, Chaki TK, Khastgir D, (2012). European Polymer Journal, 48: 1241–1248.
29. Sohi N, Rahaman M, Khastgir D, (2011). Polym Compos, 32:1148–54.
30. Pant HC, Patra MK, Negi SC, Bhatia A, Vadera SR, Kumar N (2006). Bull Mater Sci , 29:379–384.
31. Dyre J. C, (1988). J. Appl. Phys, 64(5):2456.
32. Tomara K, Suman M, Rishi Pal C and Shyam K, (2012). Synthetic Metals, 162: 820– 826.
33. Mardare D, Rusu GI and OPAPelectron J, (2004). Adv. Mater, 6(1): 333-336.
34. Paphanassiou A, (2002). J. Phys. D. Applied. Phys. 35: 17.
35. Dey A, De S and Sk D (2004). Nanotechnology. 15: 1277.
36. Elliott S. (1987). Adv. Phys. 36: 135.

CITE THIS ARTICLE AS:
Hana M Saleh and Mohammad El-Mor, Feeding Habits Of The Sharp Snout Sea Bream, *Diplodus Puntazzo* (Cetti, 1777) (Teleostei: Sparidae) From Benghazi Coast, Eastern Libya, International Journal of Bioassays, 2015, 4 (05), 3876-3887.

Source of support: Nil
Conflict of interest: None Declared